Coupling freshwater mussel ecology and river dynamics using a simplified dynamic interaction model

Amy T. Hansen[1,4], Jonathan A. Czuba[1,2,5], Jon Schwenk[1,2,6], Anthony Longjas[1,7], Mohammad Danesh-Yazdi[1,2,8], Daniel J. Hornbach[3,9], and Efi Foufoula-Georgiou[1,2,10]

[1]St Anthony Falls Laboratory and National Center for Earth-Surface Dynamics, College of Science and Engineering, University of Minnesota, 2 Third Avenue SE, Minneapolis, Minnesota 55414 USA

[2]Department of Civil, Environmental and Geo Engineering, University of Minnesota, 500 Pillsbury Drive SE, Minneapolis, Minnesota 55455 USA

[3]Departments of Environmental Studies and Biology, Macalester College, Olin-Rice Science Center, 1600 Grand Avenue, St Paul, Minnesota 55105 USA

Abstract: Freshwater faunal diversity and abundance have declined dramatically worldwide, concurrent with changes in streamflow and sediment loads in rivers. Cumulative effects and interdependencies of chronic covarying environmental stressors can obscure causal linkages that may be controlling the population dynamics of longer-lived freshwater fauna, such as mussels. To understand changes in long-term mussel population density, we developed a dynamic, process-based interaction model that couples streamflow, suspended sediment, phytoplankton, and mussel abundance under the hypothesis that chronic exposure to increased suspended sediment and food limitation are the primary factors controlling native mussel population density in a midwestern USA agricultural river basin. We calibrated and validated the model with extensive survey data from multiple time periods and used it to evaluate changes in mussel abundance at a subbasin scale over decades. We evaluated sensitivity of simulated mussel densities across a range of mortality rates and initial population densities. In scenarios representing altered sediment concentrations, such as might occur with climate or landuse-induced changes in streamflow or sediment generation rates, mussel population density showed critical threshold responses to long-term changes in suspended sediment concentration. This model of mussel population density can be used to test hypotheses about limiting factors, identify priority locations for restoration activities, and evaluate the effects of climate- or landuse-change scenarios.

Key words: Unionidae, population dynamics, suspended sediment, freshwater mussel, hydrology, streamflow, phytoplankton, model

Freshwater mussels are the most imperiled of all freshwater fauna in North America, and 70% of the ~300 native species are listed as endangered, threatened, or of special concern (Ricciardi and Rasmussen 1999, Stein et al. 2000). No single physical, chemical, or biological factor can be implicated in the massive declines in mussel population biodiversity and abundance. Instead, multiple, often interacting, environmental stressors are concurrently degrading water quality and causing declines in populations (Strayer et al. 2004, Strayer 2008, Downing et al. 2010, Haag and Williams 2013). Potential interacting factors affecting mussels include changes in hydrologic regime, sedimentation and turbidity, channel modifications, chemical pollution, such as pesticides and NH_3, substrate instability, host-fish availability, predation, zebra mussel infestation, and food limitation (Geist and Auerswald 2007, Österling et al. 2010, Peterson et al. 2011, Haag 2012 and references within, Strayer and Malcom 2012, French and Ackerman 2014).

Many stressors known to affect mussel populations (e.g., water-quality degradation, intermittent streamflow) are associated with changes in land use and streamflow that have contributed to chronically degraded environmental conditions (Strayer et al. 2004, Poff and Zimmerman 2010, Carlisle et al. 2011, Carpenter et al. 2011). A strong interaction has been reported among mussel population density, streamflow, and sediment transport conditions, including substrate instability, excess suspended sediment concentrations, and riverbed sedimentation (Brim Box and Mossa 1999, Arbuckle and Downing 2002, Allen

E-mail addresses: [4]hanse782@umn.edu; [5]czuba004@umn.edu; [6]schwe387@umn.edu; [7]alongjas@umn.edu; [8]dane0049@umn.edu; [9]hornbach@macalester.edu; [10]efi@umn.edu

DOI: 10.1086/684223. Received 5 December 2014; Accepted 24 April 2015; Published online 12 October 2015.
Freshwater Science. 2016. 35(1):200–215.

and Vaughn 2010). Streamflow and covarying environmental attributes, such as suspended sediment concentration, nutrient and phytoplankton concentration, and sediment bed load, are highly temporally variable because of storms, seasonal patterns, and interannual drought/flood conditions. Thus, single measurements of those attributes are not expected to capture the effective habitat conditions (Biggs et al. 2005, Poff and Zimmerman 2010, Ceola et al. 2013). However, population dynamics of long-lived fauna reflect a response to long-term chronic stress more than to conditions at any given time (Strayer et al. 2004).

An example of concurrent physical and biological changes can be seen in the intensively managed agricultural landscapes of the midwestern USA (Midwest) (Poole and Downing 2004, Carpenter et al. 2011, Culp et al. 2013). During the 20th century, mean annual precipitation in the Midwest increased by 10 to 20% (Karl et al. 1996) including a significant increase in heavy precipitation (Changnon and Kunkel 1995, Angel and Huff 1997). Similar to much of the Midwest, the Minnesota River Basin (MRB), our primary study site, underwent extensive changes in land use from historic prairie–wetland mosaic to >80% row-crop agriculture (Jin et al. 2013). Together, the combined effects of increased precipitation, early snowmelt, crop conversion, and increased artificial drainage (i.e., subsurface tiling and ditches) have led to observed increases in streamflows in the MRB (Novotny and Stefan 2007, Dadaser-Celik and Stefan 2009, Schottler et al. 2014). Suspended sediment loads from the MRB also have increased as evidenced by sediment core analysis in Lake Pepin. Lake Pepin, a naturally dammed fluvial lake in the Upper Mississippi River, has experienced a >10× increase in its sediment accumulation rate over the past 150 y with 80 to 90% of its sediment attributed to loading from the MRB (Kelley and Nater 2000, Engstrom et al. 2009). In concert with these hydrologic and geomorphic changes, a decline in native mussels, macroinvertebrates, and sensitive fish species has been observed in the MRB (Kirsch et al. 1985, Musser et al. 2009). The decline in mussel population abundance and species richness coincident with dramatic increases in streamflow and suspended sediment loads suggests a causative effect and that multiple stressors may be interacting dynamically in the MRB. This hypothesis is further reinforced by the fact that in the nearby St Croix River (SCR), which has seen little expansion in agriculture and no significant increases in streamflow and sediment concentrations, richness and density have been maintained at high levels (Fago and Hatch 1993, Hornbach 2001).

Recent efforts to address multicausality of mussel population decline and distribution have relied largely on multiple regression models, such as classification and regression tree models, random-forest regression, and principal component analysis (PCA), to correlate survey observations with a suite of potentially controlling variables measured within the study system (Howard and Cuffey 2003, Gangloff and Feminella 2007, Zigler et al. 2007, Steuer et al. 2008, Cao et al. 2013). Daniel and Brown (2013) extended PCA by using structural equation modeling to model linear, single-direction process interactions. At a subwatershed scale, mussel abundance has been correlated with bankfull bed shear stress, channel gradient, agricultural land use, fish host abundance, and substrate stability (Howard and Cuffey 2003, Gangloff and Feminella 2007, Cao et al. 2013, Daniel and Brown 2013). At the subreach scale, hydraulic and geomorphic variables defined at bankfull flow conditions (e.g., shear stress, Reynolds number, Froude number) have been used successfully to predict presence/absence (Zigler et al. 2007, Steuer et al. 2008, Allen and Vaughn 2010). Such multiple regression techniques are well suited to identifying stressors that do not vary much over the modeled time scale or for which population responses are acute, but are not effective for capturing the response to subcatastrophic fluctuating stressors, such as suspended sediment, chemical pollutants, and food limitation, or to nonlinear interactions among them.

Process interaction models have been suggested as potentially viable approaches to capture interactions between biota and dynamic environmental stressors (Power et al. 1995, Berg et al. 2008). This approach is distinctly different from multiple regression models, which search for (static) correlations between population survey observations and environmental variables. Instead, process interaction models start with hypothesized stressors, and then allow the model variables to evolve through time to predict population characteristics, which are compared to survey observations. This approach has not yet been widely used for predicting mussel abundance because of the extensive amount of input information required from basic experimental research to define the relevant processes, parameters, and variables. For example, Berg et al. (2008) proposed such a model that included all life stages but faced challenges in estimating the model parameters because of the scarcity of information regarding critical population and life-history characteristics for nonadult life stages. Process interaction models are especially well suited to guide population or watershed management under uncertain conditions, such as climate or landuse change (Cuddington et al. 2013), because they capture dynamic changes in variables or interactions among variables.

We present a process-based dynamic interaction model that can be used to test the predictive power of a model that captures the cumulative effects of fluctuating environmental conditions on the population density of long-lived, sedentary aquatic organisms, i.e., freshwater mussels. The model makes many simplifying assumptions, such as generic mussel behavior and growth parameters and limited environmental variables, to explore the plausibility of predicting mussel density over space. The primary under-

lying assumption of the model is that increasing streamflow magnitude and fluctuations are controlling long-term aggregate mussel population density through increased suspended sediment concentrations and food limitation in agricultural watersheds (Fig. 1). The nonlinear interactions of the model variables (streamflow, suspended sediment, phytoplankton, and freshwater mussel density) at short time scales (daily) are integrated within the model across a much longer time scale (decades).

If the model cannot explain the spatial distribution of mussel density or the change in density over time, then its hypotheses failed to capture either the correct variables or the interactions and must be adjusted. If the model predictions agree with the observed trends, then it supports our conceptual understanding of the 1st-order controls on the system dynamics and can be used in 3 complementary modes: 1) as a predictive tool to assess the response of the system to future changes, 2) as a decision management tool to explore locations and actions for restoration activities, and 3) as an exploratory tool to suggest critical areas and times where better data collection would further refine and parameterize the model for increased prediction accuracy.

METHODS

Model development

The model is based on processes and interactions that we hypothesize to act as 1st-order controls on the spatial and temporal variability of mussel density throughout the MRB and SCR (Fig. 2). Driven by streamflow (Q_t; L/s), the 3 dependent variables, inorganic suspended sediment concentration (S_t; g/L), phytoplankton population density represented by chlorophyll *a* concentration (C_t; g/L), and multispecies mussel population density (M_t; mussels/m^2) co-evolve and interact through time. These 4 variables are updated using empirical and theoretical functional relationships on a daily time step for a period of multiple decades. The model is deterministic, and we derived fixed parameters from the literature or, when possible, from site-specific data (summarized in Table 1, details in Appendices S1, S2). We selected 2 parameters, initial mussel density (M_0) and mortality rate (ε_M), for model calibration using survey data from 12 sites in the upper Midwest. The model was validated with survey data from 4 of these 12 sites collected on earlier dates.

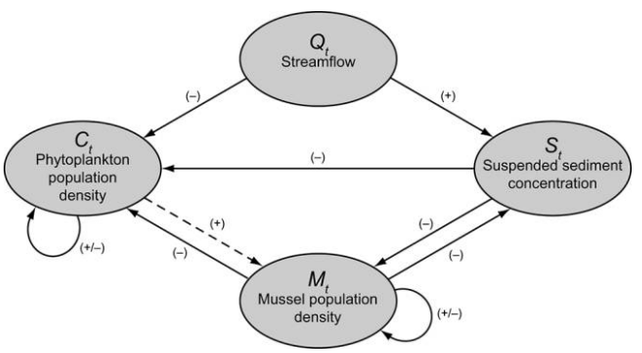

Figure 1. Process interaction network showing the coupled hydrogeobiological system that is incorporated into the dynamic model and applied to the Minnesota River Basin and St Croix River. Dashed lines show weak interactions, and solid lines show strong interactions, which are either positive (+) or negative (–). Driven by Q_t, the coupled interaction relationships are expressed via Eqs 4–6. The subscript t indicates time.

The general form of the model can be expressed by the following set of coupled, nonlinear differential equations:

$$\frac{dS_t}{dt} = f(S_t, M_t, Q_t), \quad \text{(Eq. 1)}$$

$$\frac{dC_t}{dt} = f(C_t, M_t, S_t, Q_t), \quad \text{(Eq. 2)}$$

$$\frac{dM_t}{dt} = f(M_t, C_t, S_t). \quad \text{(Eq. 3)}$$

Assuming initial conditions S_0, C_0, M_0, and given a time series of daily streamflow data (Q_t), which acts as the forcing variable, the above set of equations dynamically couple these variables exerting process interactions and feedbacks to generate daily time series of S_t, C_t, and M_t at each location where the model is applied. No explicit spatial scale exists because the variables are concentrations. The general relationships given in Eqs 1–3 incorporate known functional dependencies of sources and sinks and modulated population growth models. We parameterize these relationships as:

$$\frac{dS_t}{dt} = f_1(Q_t) - f_2(M_t, S_t, Q_t)S_t, \quad \text{(Eq. 4)}$$

where $f_1(Q_t)$ is the flow-dependent suspended sediment generation rate and $f_2(M_t, S_t, Q_t)$ is the mussel filtration rate,

$$\frac{dC_t}{dt} = f_3(S_t)C_t\left(1-\frac{C_t}{K_C}\right) - \left(f_4(Q_t) + f_2(M_t, S_t, Q_t)\right)C_t, \quad \text{(Eq. 5)}$$

where $f_3(S_t)$ is the sediment-modulated phytoplankton growth rate, $C_t\left(1-\frac{C_t}{K_C}\right)$ is logistic growth of the phytoplankton with carrying capacity (K_C), and $f_4(Q_t)$ describes streamflow dilution of phytoplankton, and

$$\frac{dM_t}{dt} = f_5(S_t)M_t\left(1-\frac{M_t}{f_6(C_t)}\right), \quad \text{(Eq. 6)}$$

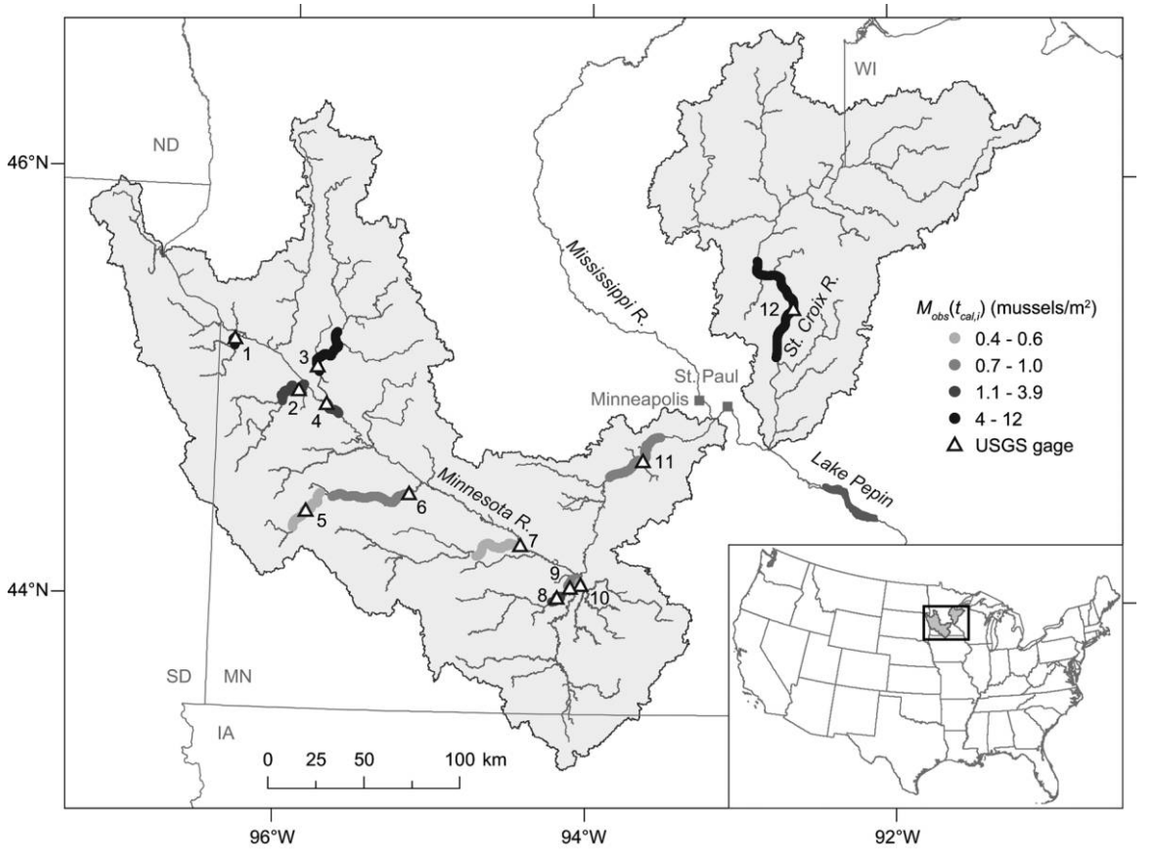

Figure 2. Map of the Minnesota River Basin (MRB) and the St Croix River Basin (SCR) where a dynamic interaction model was applied. Sufficient physical and biological data were available for 12 reaches. Triangles show the location of US Geological Survey (USGS) streamflow gages and monitoring stations. Numbers correspond to individual sites as listed in Table 2. Thick lines show the extent over which mussel survey results were averaged, and the line shading indicates observed site-specific mussel density ($M_{obs}[t_{cal,i}]$) as shown in the legend. ND = North Dakota, SD = South Dakota, MN = Minnesota, WI = Wisconsin, R = river.

where $f_5(S_t)$ is the sediment-modulated mussel population growth and $M_t(1-\frac{M_t}{f_6(C_t)})$ is logistic growth of the mussel population with food-modified effective carrying capacity.

Functional interactions Flow-dependent suspended sediment generation $f_1(Q_t)$ is typically assumed to have a power law relationship (e.g., Leopold et al. 1964):

$$f_1(Q_t) = \alpha_{QS} Q_t^{\beta_{QS}}, \qquad \text{(Eq. 7)}$$

where α_{QS} and β_{QS} are constants that were estimated from site-specific Q_t and suspended sediment-monitoring data (USGS 2014) (see Table S1 for the fitted parameters and Fig. 3A). Within the model, the change in S_t caused by Q_t was modeled as the difference between Eq. 7 at t and at $t + 1$ divided by dt. This relationship was significant at all sites ($p < 0.001$), but the predictive power varied from site to site with a range in R^2 from 0.21 to 0.75 and median $R^2 = 0.38$. For some sites, we made modifications to invoke this relationship only above a critical Q_t, whereas for lower Q_t values, S_t was a constant value estimated from observations (Table S1).

The effect of mussel filtration on S_t and C_t is reflected in the model in Eqs 4 and 5 through $f_2(M_t, S_t, Q_t)$:

$$f_2(M_t, S_t, Q_t) = \frac{R_{C,t} w_M}{d_t} M_t, \qquad \text{(Eq. 8)}$$

where $R_{C,t}$ (L h^{-1} g^{-1}) is the mussel clearance rate normalized by mussel wet mass (Fig. 4A), w_M (g/mussel) is the site-specific average wet mass (described further in Appendix S1), and d_t (m) is the average stream depth (Fig. 3B):

$$d_t = \alpha_{Qd} Q_t^{\beta_{Qd}}, \qquad \text{(Eq. 9)}$$

where α_{Qd} and β_{Qd} are site-specific constants that were determined by regression of simultaneous Q_t and d_t, computed as measured channel area over measured channel top width from monitoring data (USGS 2014) (Table S2, Fig. 3B).

Table 1. Summary of model parameters whose values were set based on available literature. C = phytoplankton population density, S = suspended sediment concentration, M = mussel, R = mussel clearance rate.

Parameter	Description	Value	Reference
b_M	Juvenile mussel recruitment rate	1.3/y	Haag 2012
C^*_M	Modifies K_C to set food limitation onset	0.5	Not available in literature
K_C	Phytoplankton carrying capacity	0.4 mg/L	Sarnelle 1992, MPCA 2013
K_M	Mussel carrying capacity	26.2 mussels/m^2	Hornbach et al. 2010
r_C	Phytoplankton population growth rate	390/y	Nielsen et al. 1996, Marañón et al. 2013
R^*_C	Parameter relating mussel clearance rate to S_t	0.087 L/mg	Regression to results reported in literature[b]
$R_{C,max}$	Maximum mussel clearance rate	0.066 L h^{-1} g^{-1}	Regression to results reported in literature[b]
S^*_C	Maximum S where r_C is not affected by S	420 mg/L	Schallenberg and Burns 2004[a]
S^*_M	Maximum S where b_M is not affected by S	10 mg/L	Österling et al. 2010[a]; Gascho Landis et al. 2013
$S_{M,max}$	Suspended sediment concentration where $b_M = 0$	50 mg/L	Gascho Landis et al. 2013
$S_{C,max}$	Suspended sediment concentration where $r_C = 0$	1760 mg/L	Stefan et al. 1983

[a] Reported as turbidity (NTU) and converted to suspended sediment concentration using empirically derived relationships based on Minnesota River monitoring data at multiple sites; S (mg/L) = 2.1(NTU)

[b] Observations of mussel clearance rate at known suspended solid concentrations used for the exponential decay function in model from Kryger and Riisgård 1988, Ogilvie and Mitchell 1995, Baker and Hornbach 2001, Pusch et al. 2001, Gascho Landis et al. 2013

$R_{C,t}$ is the volume of water cleared of particles per unit time per mussel and decreases with increasing S_t (Alimov 1981, Hornbach et al. 1984, Gascho Landis et al. 2013). $R_{C,t}$ is modeled as an exponentially decaying function dependent on S_t:

$$R_{C,t} = R_{C,\max}\, e^{-R^*_C S_t}, \qquad \text{(Eq. 10)}$$

where the 2 parameters, $R_{C,max}$ (L g^{-1} h^{-1}) and R^*_C (L/g) were estimated from a least-squares regression of Eq. 10 to observed clearance rates at suspended solid concentrations reported in the literature (R^2 = 0.58, n = 16, p = 0.0006; Fig. 4A; Kryger and Riisgård 1988, Ogilvie and Mitchell 1995, Baker and Hornbach 2001, Pusch et al. 2001, Gascho Landis et al. 2013).

Phytoplankton growth modulated by S_t in Eq. 5 is represented in the model with a threshold-driven functional relationship $f_3(S_t)$ as

$$\begin{aligned} f_3(S_t) &= r_C && \text{for } S_t \le S^*_C \\ &= r_C\left[\frac{S_{C,max}-S_t}{S_{C,max}-S^*_C}\right] && \text{for } S_t > S^*_C, \end{aligned} \qquad \text{(Eq. 11)}$$

where r_C (1/y) is the maximum population growth rate (i.e., birth rate – death rate), S^*_C [g/L] is the threshold in S_t above which S_t adversely effects phytoplankton growth rate (Schallenberg and Burns 2004), and $S_{C,max}$ (g/L) is the suspended sediment concentration at which no population growth occurs (Stefan et al. 1983; Fig. 4B).

Streamflow dilution of phytoplankton is incorporated in the model in Eq. 5 with the function $f_4(Q_t)$:

$$f_4(Q_t) = \frac{1}{Q_t}\frac{dQ_t}{dt}. \qquad \text{(Eq. 12)}$$

This form is supported by the observed inverse relationship between C and Q, as expected from dilution, in the monitoring data at MN-Jordan (site 11) on the Minnesota River (MPCA 2013).

The effective mussel population growth rate, i.e., the growth rate modulated by a function of S_t, is represented in the model by $f_5(S_t)$, where

$$\begin{aligned} f_5(S_t) &= b_M - \varepsilon_M && \text{for } S_t \le S^*_M \\ &= \left[\frac{S_{M,max}-S_t}{S_{M,max}-S^*_M}\right] b_M - \varepsilon_M && \text{for } S^*_M < S_t < S_{M,max} \\ &= -\varepsilon_M && \text{for } S_t \ge S_{M,max}. \end{aligned} \qquad \text{(Eq. 13)}$$

In the above expressions, b_M (1/y) is the juvenile recruitment rate, ε_M (1/y) is the mortality rate, $S_{M,max}$ (g/L) is the S_t at which the juvenile recruitment rate is 0, and S^*_M (g/L) is a threshold below which S_t does not limit juvenile recruitment (Fig. 4C). Suspended sediment can reduce the number of gravid females and can cause recruitment failure above a threshold concentration (Österling et al. 2010, Gascho Landis et al. 2013). The juvenile life-history stage is assumed to limit overall population growth (Daraio et al. 2010, Arvidsson et al. 2012, French and Ackerman 2014).

The effective mussel carrying capacity, $f_6(C_t)$, is modeled by a threshold relationship that is modulated by food availability.

$$f_6(C_t) = \left[\left(\frac{C^*_M}{K_C}\right)C_t + C^*_M\right]K_M \quad \text{for } C_t < K_C, \qquad \text{(Eq. 14)}$$

where K_M [mussels/m^2] is the nominal carrying capacity and C^*_M modifies K_C to set the phytoplankton population

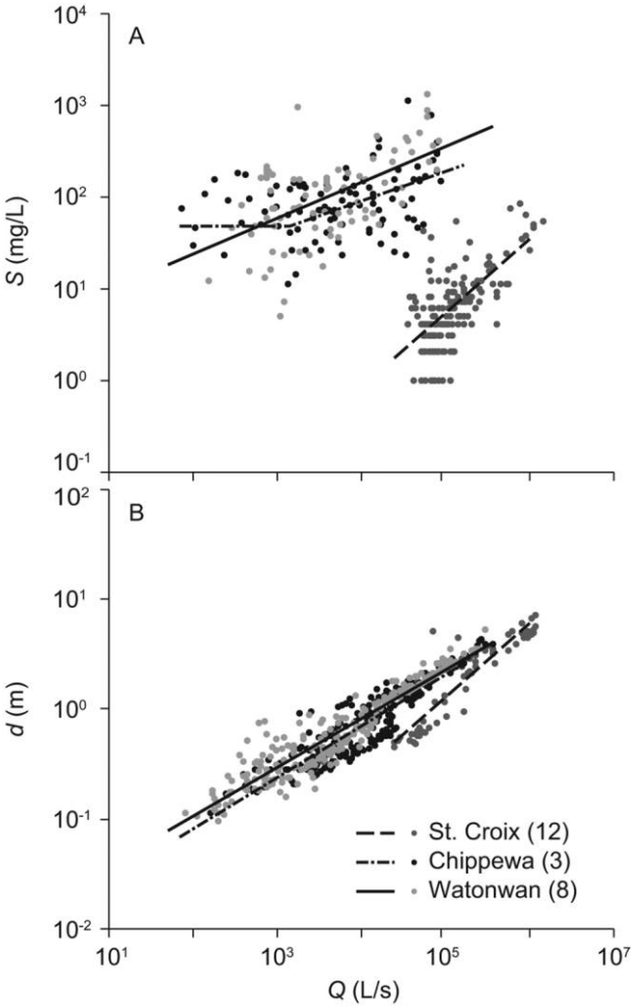

Figure 3. Empirical relationships between daily streamflow (Q) and measured suspended sediment concentration (S; Eq. 7, Table S1) (A) and depth (d; Eq. 9, Table S2) (B) used in model parameterization and observational data from US Geological Survey (USGS) gaging stations for the 3 sites used as examples throughout the paper (St Croix [12], Chippewa [3], and Watonwan [8]). USGS observational data are shown as points, and lines represent the empirical relationships derived from the regression of Eqs 7 and 9 to the observational data. The extent of each line along the x-axis corresponds to the range of measured Q_t for each site.

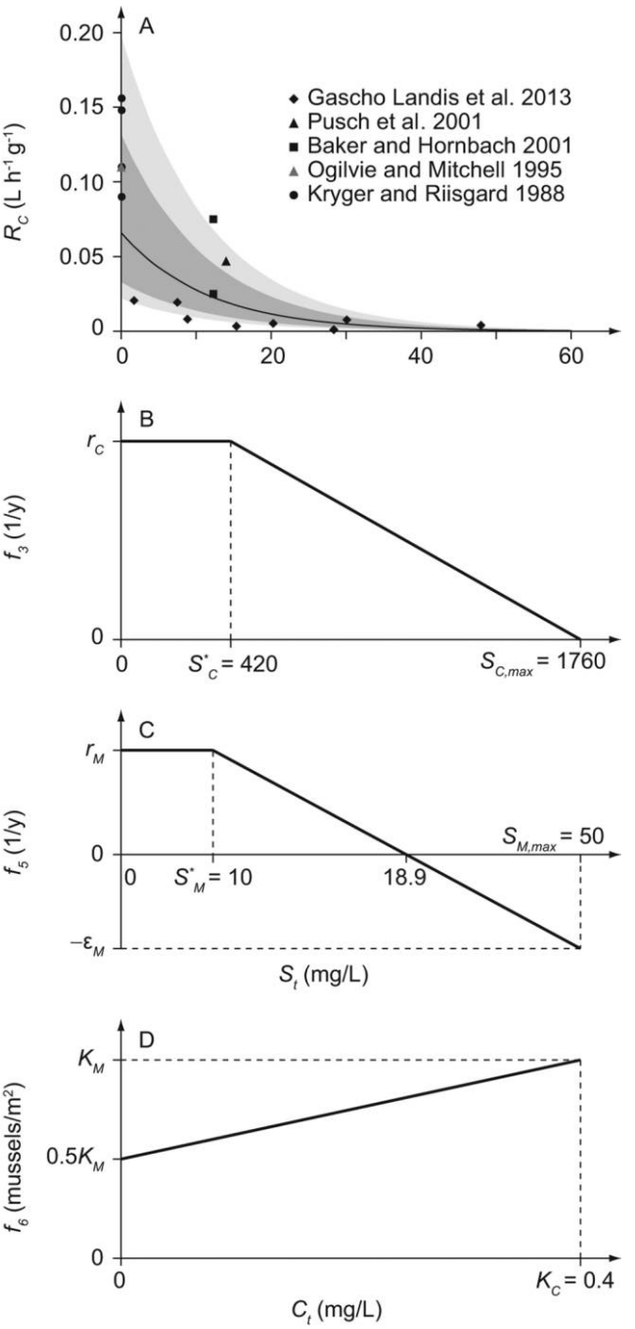

Figure 4. Functional interactions between mussel clearance rate (R_C; Eq. 10) (A), effective phytoplankton population growth rate ($f_3[S_t]$; Eq. 11) (B), and effective mussel population growth rate ($f_5[S_t]$; Eq. 13) (C) as a function of suspended sediment concentration (S_t) and effective mussel population carrying capacity ($f_6[C_t]$; Eq. 14) as a function of phytoplankton population density as chlorophyll a concentration (C_t) (D). In panel A, the line shows the relationship used in model development. Symbols show values reported in the literature. The dark gray region shows R_C between 0.5 and 2× the modeled R_C, and the light gray region shows R_C between 0.25 and 4× the modeled R_C. See Table 1 for parameter abbreviations, values, and sources.

density where food limitation alters the maximum number of mussels that can be sustained at a site (Fig. 4D).

Model parameterization The model has 16 prescribed parameters, 11 of which were set by values reported in the literature (Table 1). The remaining 5 (α_{Qd}, β_{Qd}, α_{QS}, β_{QS}, and w_M) were estimated with site-specific data (see Appendix S1 for a detailed discussion). Two additional parameters, ε_M and M_0 in 1976, were estimated via calibration.

Study sites

We applied our model to 11 sites within the MRB and 1 site in the SCR (Fig. 2). The MRB is primarily used for agriculture with ~80% row-crop agricultural land use (Jin et al. 2013). The SCR sustains more diverse land use of 23% cropland, 28% rangeland, and 25% forest/shrub (Fago and Hatch 1993, Donatell et al. 2014). Of the 41 native mussel species reported in historical records only 23 species are currently found in the MRB, and 9 of those are now rarely found (Musser et al. 2009). In contrast, the SCR is considered excellent mussel habitat with 41 living mussel species and some of the highest density and diversity found in Minnesota (Hornbach 2001).

We included in the calibration and validation site list all river reaches in the 2 basins for which sufficient physical and biological observations were available. Physical information required to apply the model was: ≥18-y record of Q_t, channel measurements needed to estimate the parameters α_{Qd} and β_{Qd} of the Q_t–d_t relationship (Eq. 9), and S_t measurements to estimate the parameters α_{QS} and β_{QS} of the Q_t–S_t relationship (Eq. 7). Three reaches exhibited no significant Q_t–S_t relationship, leaving 12 viable sites in the MRB or SCR (Fig. 2). For the 12 sites, reach-averaged observed population density (M_{obs}) was defined as the average population density from all survey observations collected at locations that satisfied the following conditions: 1) in the same river reach as the streamflow gage, 2) ≤20 km of the gage, and 3) not up- or downstream of major tributaries (population density and spatial extent of the sites are shown in Fig. 2).

Observations of mussel populations

Mussel population diversity and abundance in the MRB and SCR have been quantified twice. In 1989–1991, quadrat transects and timed surveys were completed in the mainstem Minnesota River, the Chippewa River, and the SCR. The 1989–1991 data consisted of results from 3 independent surveys: 888 live mussels representing 33 species were found at 9 sites on the SCR (Hornbach 1991), 1268 live mussels representing 20 species were found at 59 sites on the Minnesota River (Bright et al. 1990), and 4090 live mussels representing 21 species were found at 32 sites on the Chippewa River (Bright et al. 1995). Further details on the sampling methods for the 1989–1991 surveys are contained in the original references. The 1999–2012 observations consisted of timed surveys throughout the MRB and the SCR, which were made available to us by the Natural Heritage and Nongame Research Program of the Division of Ecological Services, Minnesota Department of Natural Resources (MN DNR, current as of 10 May 2013). In the 1999–2012 survey, 27,531 live mussels representing 21 species were found at 478 locations within the MRB, and 4077 live mussels representing 29 species were found at 89 survey locations on the SCR. Survey locations were chosen for ease of access and, for most locations, the survey crew had no prior knowledge of populations (B. Sietman, MN DNR, personal communication). Average search time per site was 104 min with a range of 30 to 240 min. On average and across all surveyed sites, 40% of all collected mussels were in the 0–5 age class indicating that active recruitment was occurring within the MRB and that the populations are not relict. For all species collected, some juveniles were found. Further details on the 1999–2012 survey method and data can be obtained through direct contact with the MN DNR (info.dnr@state.mn.us).

Model calibration and validation

We calibrated the model on 2 parameters related to mussel population growth: ε_M and M_0. Species-specific mortality rates are available in the literature for some species, but mussel assemblages are composed of many species, so we calibrated on an ε_M that represented the assemblage average (Newton et al. 2011, earlier references synthesized by Haag 2012). The 2nd calibration parameter, M_0, was not available. During the calibration process, we allowed ε_M to range from 0.19 to 1.9/y and M_0 to range from 0.1 to 10 mussels/m^2. We selected the calibrated values ε_M* and M_0* as those values that minimized the root mean square error (RMSE) between observed population densities ($M_{obs}[t_{cal,i}]$), as reported in the 1999–2012 data set, and simulated population densities ($M_{sim}[t_{cal,i}]$), both evaluated on the site-specific observation date ($t_{cal,i}$) across all sites. For each site, we ran the model using the daily observations of Q_t from 1 September 1976 to the site-specific survey observation date (Table 2). We updated S_t, C_t, and M_t daily throughout this period across the entire range of ε_M and M_0 values. We used the data set with observations from more sites, i.e., the MN DNR survey data, for calibration to constrain the model adequately. We examined model sensitivity to the calibrated parameters $M0$ and ε_M over realistic ranges.

Model validation consisted of comparing $M_{obs}(t_{val,i})$ with the $M_{sim}(t_{val,i})$, and then computing the R^2 value of the linear regression across all sites. The survey observations used for model validation consisted of independent mussel density observations from surveys during 1989–1991 at the 4 sites with sufficient S_t and Q_t data.

The survey methods for quantifying M_t in the field varied between the 2 periods considered, and we made an effort to adjust for this factor. We converted the 1999–2012 observations, which were semiquantitative and reported as catch per unit effort (CPUE), to population density (mussel/m^2) using a linear regression developed from the semiquantitative and quantitative survey observations by Bright et al. (1990, 1995) ($M_{density} = 0.0712M_{CPUE}$, $R^2 = 0.61$, $n = 40$, $p < 0.0001$). Semiquantitative sampling involves counting and classifying all individuals encountered at a location over a specified period of time. In contrast, quantitative

Table 2. Site information including site name and number, survey dates for mussel population observations, and site-specific, site-averaged mussel wet mass (w_M). Values in parentheses are used in model application and are an average of the observations. Sites are listed from west to east.

Site name	Actual survey dates (dates used for model calibration)	Actual survey and model validation dates	w_M range (value used for model) (g)
1. Yellow Bank	June 2000 (30 September 1999)[a]	–	30.0–339.0 (73.9)
2. Lac Qui Parle	June 2000 (30 September 1999)[a]	–	4.9–339.0 (78.1)
3. Chippewa	June 2008, July 2008 (15 July 2008)	1 July 1989	15.7–339.0 (121.2)
4. MN-Montevideo	August 2006 (20 August 2006)	1 July 1989	15.7–339.0 (67.0)
5. Redwood-Marshall	September–October 2000 (18 September 2000)	–	30.0–339.0 (148.4)
6. Redwood-R. Falls	October 2000, July 2002 (31 August 2001)	–	30.0–339.0 (85.0)
7. Cottonwood	July 2002, July 2003 (18 January 2003)	–	34.4–339.0 (150.7)
8. Watonwan	September–October 1999 (22 September 1999)	–	34.4–339.0 (227.3)
9. Blue Earth	September 2000 (18 September 2000)	–	15.7–339.0 (159.9)
10. Le Sueur	September 1999 (22 September 1999)	–	53.2–236.3 (175.2)
11. MN-Jordan	Sept 2000, 2001, 2008, Oct 2003, Aug 2006 (7 March 2005)	1 July 1989	15.7–339.0 (101.0)
12. St Croix	July 2009, 2010, 2011, Sept 2011, 2012 (8 June 2011)	1 January 1991	15.7–339.0 (85.2)

[a] Streamflow record ended 30 September 1999

sampling consists of counting and classifying all mussels encountered within uniformly spaced quadrats along transects and includes removing and sieving the sediment to a fixed depth. Semiquantitative sampling tends to underestimate small size classes, does not count burrowed mussels, can underrepresent species richness if the sampling effort is not for a long enough duration, or can overrepresent abundance by targeting known beds (Hornbach and Deneka 1996, Smith 2006). The linear relationship between CPUE and mussels/m^2 as developed from the Bright et al. (1990, 1995) data suggests that semiquantitative sampling, although not an absolute measure of abundance, provides consistent relative estimates of mussel density across all sampled sites.

Scenario simulations

We created scenarios to evaluate M_t responses to changes in sediment generation rate by linearly scaling α_{QS} (Eq. 7), such that the long-term averaged suspended sediment concentration ($S_{t,avg}$) varied from 0.1 to 100 mg/L, or by linearly scaling Q_t, which preserved the variability but shifted the mean. Changes in sediment generation rate via α_{QS} could result from changes in bank stability or upland erosion rates, whereas changes in Q_t could result from climate-induced precipitation changes or from changes in watershed land use. We ran the model from 1 September 1976 to 30 September 2012 to evaluate scenario responses.

We tested the effect of selected processes on the model predictive ability by running simplified versions of the model and comparing the subsequent simulation results to the calibration survey observations. First, we tested for a direct Q_t–S_t interaction without mussel feedback for predictability through linear regression of M_{cal} to a site-specific $S_{t,avg}$ where flow-modulated sediment generation was computed from Eq. 7 for each site then averaged across the time period from the model initiation to the calibration date. Second, we deactivated mussel filtration by setting $f_2(M_m, S_t, Q_t) = 0$ (Eq. 8) to evaluate the effectiveness of filtration at promoting self-survival. We examined the effect of food limitation by setting $f_6(C_t) = K_M$ in the calibrated model and compared the simulated population density to that predicted with food limitation included.

RESULTS

Calibration and validation

Calibration yielded $\varepsilon_M{}^* = 1.01$/y and $M_0{}^* = 0.7$ mussels/m^2 (RMSE = 1.46 mussels/m^2, $R^2 = 0.89$, $n = 12$, $p < 0.001$; Fig. 5A). A narrow band of low RMSE was obtained for a range of values of ε_M and M_0 (Fig. 5B). For low initial population density ($M_0 < \sim 1.5$ mussel/m^2), the model was sensitive to both ε_M and M_0. Model sensitivity to M_0 decreased as M_0 increased ($M_0 > \sim 1.5$ mussel/m^2), whereas the model was sensitive to ε_M across its entire range. The insensitivity to initial conditions implies a sufficient time interval for the simulated populations at each site to dynamically correct from errors introduced from the specification of a uniform value of M_0 for all sites. For model validation, $M_{sim}(t_{val,i})$ was compared to the $M_{obs}(t_{val,i})$. The model was able to reasonably predict population density, although based on a limited number of validation sites (RMSE = 1.43 mussels/m^2, $R^2 = 0.94$, $n = 4$, $p = 0.030$; Fig. 5A).

Mussel population sensitivity

With M_0 fixed at the calibration value $M_0{}^* = 0.7$ mussels/m^2, simulated population densities approached either

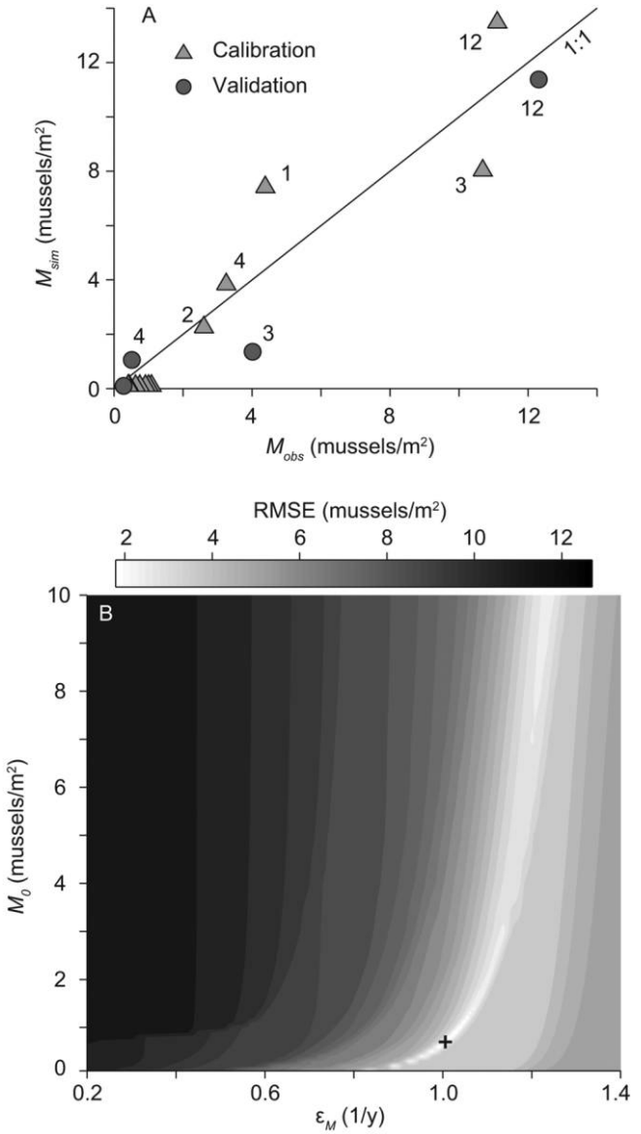

Figure 5. A.—Calibration and validation of simulated mussel population densities (M_{sim}) against their corresponding observed values. Numbers refer to site number (Table 2). B.—Contour plot of root mean square error (RMSE) for 12 calibration sites across the considered range of mussel mortality rates (ε_M) and initial mussel population density (M_0). Lighter shades correspond to smaller error, and the change in gradation shows model sensitivity. A narrow band of low RMSE was obtained for a range of values of ε_M and M_0. The calibrated parameter/initial condition (*) is denoted by + ($\varepsilon_M{}^* = 1.01$/y and $M_0{}^* = 0.7$ mussels/m^2; RMSE = 1.46 mussels/m^2, $n = 12$).

0 or the effective K_M, corresponding to the fixed points of the logistic equation governing population growth (Eq. 6, Fig. 6A). While all sites shared the same final population density for extirpation conditions (i.e., ≈ 0 mussel/m2), the equilibrium state related to K_M was modulated by food availability, as accounted for by function f_6 (Eq. 14), and varied between sites. Between 0 and the effective K_M, $M_{sim}(t_{cal,i})$ responded dynamically to modeled interactions (Fig. 6A). This dynamic region is shown shaded on Fig. 6A for the 3 example sites; St Croix (site 12), Chippewa (site 3), and Watonwan (site 8), which span a range of environmental stressors and mussel population responses. We will use these sites illustratively throughout the results section.

For different sites, the region of dynamic population response occurs at different ranges of ε_M and illustrates how environmental stressors can suppress mussel population growth (Fig. 6A). For instance at St Croix (12), the simulated environmental stressors are so minimal that ε_M must approach the nominal recruitment rate before $M_{sim}(t_{cal,i})$ moves away from the asymptote at effective carrying capacity (Fig. 6A). In contrast, environmental stressors at Watonwan (8) strongly affect recruitment and mussel populations grow only if ε_M is very low. At the calibrated ε_M and M_0 (vertical line and +; Fig. 6A, B), the Chippewa (3) population was within the dynamic response region, the St Croix (12) population was approaching its effective carrying capacity, and the simulated Watonwan (8) population was near extirpation. Within the full calibration parameter space, the region of dynamic response for individual sites converged as M_0 increased and for a small range in ε_M (Fig. 6B). Results in Fig. 6B are consistent with Fig. 5B and show that the dynamic response region is relatively sensitive to changes in ε_M and insensitive to the initial condition for $M_0 > \sim 1.5$ mussel/m^2.

We explored sensitivity of the model to the fixed parameters K_M, R_C, and w_M by varying each parameter independently and comparing $M_{sim}(t_{cal,i})$ to $M_{obs}(t_{cal,i})$. Model predictability of M_t was insensitive to K_M. Across a range of K_M from 11 to 26 mussels/m^2, the regression coefficient (R^2) between simulated and observed density, evaluated on the calibration dates at the 12 calibration sites, ranged from 0.86 to 0.89. Changes in K_M shifted effective carrying capacity, which affected model predictions only at sites approaching K_M, such as St Croix (12). We tested model sensitivity to R_C by applying a linear multiplier to the modeled functional dependence of R_C on S_t (Eq. 4; ranges shown as shaded regions in Fig. 4A). R_C varies by season, species, and burrowing behavior, which introduce inherent uncertainty to this fixed parameter (Amyot and Downing 1997, Watters et al. 2001, Allen and Vaughn 2010). The model was sensitive to reductions in R_C. Varying the value of R_C within a range of $\frac{1}{3}R_C$ to $\frac{1}{2}R_C$, decreased the R^2 from 0.89 to 0.45, and the model predicted extirpation at 10 of the 12 sites. The model was less sensitive to increases in R_C. Doubling R_C resulted in model predictability with $R^2 = 0.68$ and tripling R_C resulted in $R^2 = 0.57$. We also examined model sensitivity to w_M by applying the average w_M to all sites. The assumptions regarding average age and size used to estimate the site-specific w_M are described in detail in Appendix S1. When

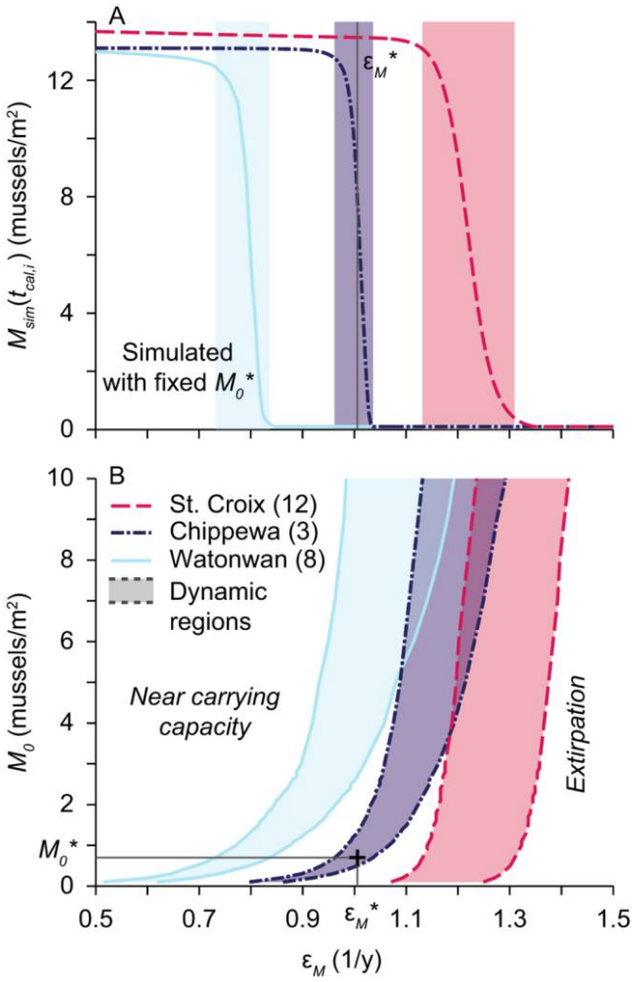

Figure 6. A.—Sensitivity of simulated mussel population density ($M_{sim}[t_{cal,i}]$) to mussel mortality rate (ε_M) (evaluated at the calibrated M_0^* = 0.7 mussels/m^2). Each line represents $M_{sim}(t_{cal,i})$ evaluated at its corresponding calibration date for a range of εM. The vertical line denotes the calibrated mortality rate (ε_M^*). Shading shows the range of ε_M for which $M_{sim}(t_{cal}i)$ is most responsive to changes in ε_M. B.—Zones of dynamic mussel population response (shaded areas) for 3 example sites across the calibration parameter space. To the left of the shaded region, mussel density (M_t) is approaching the effective carrying capacity ($f_6[C_t]$; Eq. 14), to the right of the shaded region, mussels are predicted to be extirpated. + denotes the calibrated value of M_0^* and ε_M^*.

run with a constant w_M for all sites, the average across-sites value of w_M = 100 g, comparison of $M_{sim}(t_{cal,i})$ with $M_{obs}(t_{cal,i})$ resulted in an R^2 = 0.38. Conversely, preserving site variability by applying a linear multiplier to w_M had a much smaller effect on model predictability. For a 10% increase in w_M at all sites, R^2 = 0.85, and for a 10% decrease, R^2 = 0.74.

Temporal model dynamics

Changes in Q_t, the driving variable, and its propagation through dynamic process interactions with S_t, C_t, and M_t, are reflected in the time series for each variable (Fig. 7A–D). The simulated change over time of M_t was markedly different at the 3 example sites but was not visually discernible from temporal patterns in any of the interdependent environmental variables (Q_t, S_t, C_t). For example, St Croix (12) had the highest Q_t of the 3 sites but the lowest S_t. Chippewa (3) and Watonwan (8) had similar Q_t and C_t, but very different S_t, with Watonwan (8) S_t approximately an order of magnitude higher than Chippewa (3). The subsequent simulated mussel population at Watonwan (8) was never able to escape the limitations on recruitment imposed by S_t, whereas for the same growth parameters at Chippewa (3), the mussel population steadily rose until only food availability was limiting growth. Similar to Chippewa (3), the simulated mussel population at St Croix (12) was limited primarily by food availability and approached effective carrying capacity.

Three of the 12 calibration sites generally had increasing simulated temporal trajectories in M_t, 2 sites fluctuated near the initial condition, and 7 sites fluctuated around 0.1 mussels/m^2 (the minimum density predicted by the model) (Fig. 8). Four sites have been surveyed more than once (Chippewa [3], MN-Montevideo [4], MN-Jordan [11], and St Croix [12]). The model correctly predicted the observed population trends at Chippewa (3), MN-Montevideo (4), and MN-Jordan (11), but did not capture the observed trend of declining M_t at St Croix (12). The low predictive ability at St Croix (12) indicates that modified functional relationships or parameters may be needed to capture feedbacks at that site.

Nonlinear interactions

The importance of the processes incorporated into the model for the predictability of M_t was tested by removing process links then comparing the simulated M_t from the partial model with the full model simulation. First, a direct Q–S interaction without mussel feedback was tested for predictability by analyzing the correlation between M_t and $S_{t,avg}$. The predicted $S_{t,avg}$ from 1976 to the $t_{cal,i}$ survey date was correlated with M_t (R^2 = 0.48, n = 12, p = 0.013), consistent with the hypothesis that elevated S_t and higher Q_t adversely affect M_t.

Next, when the mussel filtration process was deactivated (by setting Eq. 8 equal to 0), mussels were predicted to be extirpated at 10 of the 12 sites. At St Croix (12), simulated M_t was predicted to be higher with filtration deactivated indicating that self-limitation because of food availability is the controlling process at this site. In contrast, with mussel filtration of suspended solids acti-

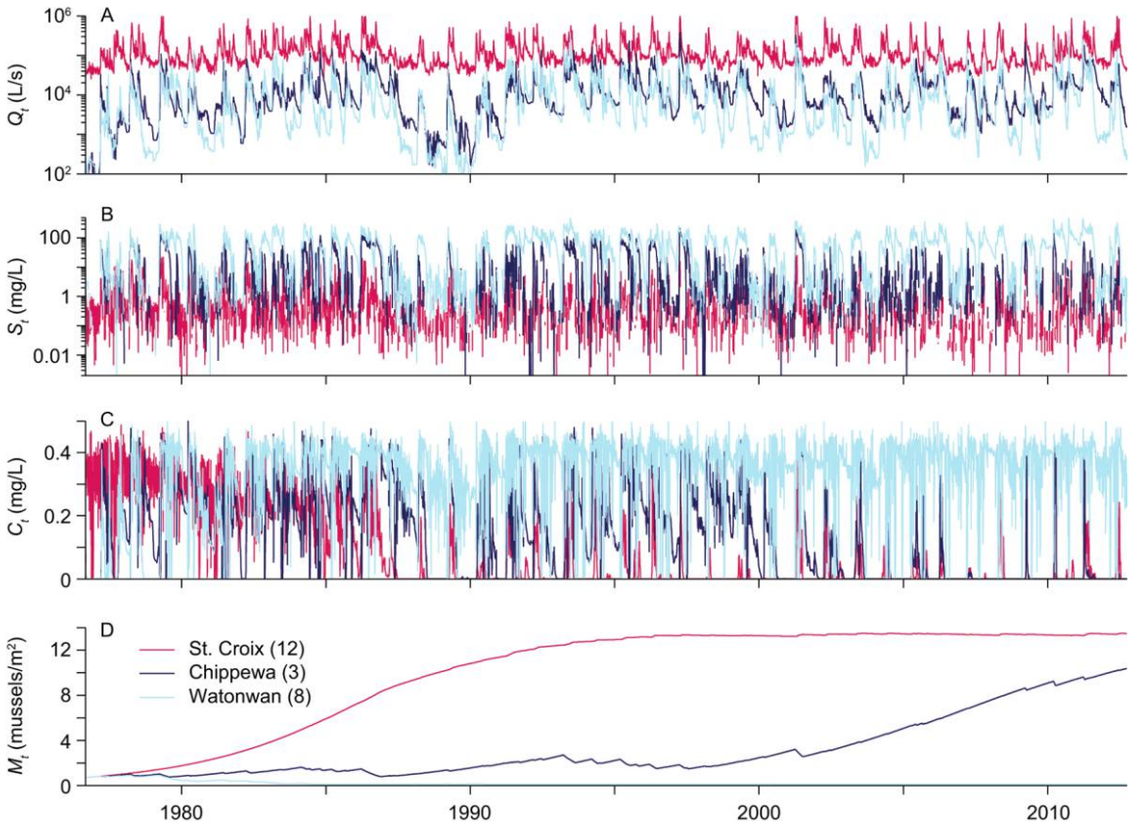

Figure 7. Temporal variability in US Geological Survey measured streamflow (Q_t) (A) and the interdependent simulated variables suspended sediment concentration (S_t) (B), phytoplankton population density (C_t) (C), and mussel population density (M_t) (D) for 3 of the 12 sites.

vated, i.e., running the full model, the simulation results corresponded better with observations and extirpation was predicted at 7 sites, consistent with extremely low densities reported in the calibration survey observations.

When food limitation was removed from the model (i.e., by setting $f_6 = K_M$ in Eq. 14), sites with $M_{sim}(t_{cal,i}) < 4$ mussels/m^2 were not affected. However, at sites with $M_{sim}(t_{cal,i}) > 4$ mussels/m^2 (Yellow Bank [1], Lac Qui Parle [2], Chippewa [3], MN-Montevideo [4], St Croix [12]), food limitation accounted for as much as a 49% reduction in simulated M_t with the largest effect at the sites with the highest M_t. Similar to changes in the K_M, food limitation shifted the magnitude of M_t but did not change the dynamic behavior at any individual site nor change the model predictability across all sites ($R^2 = 0.87$).

Mussel population response to changing environmental stressors

Scenarios of differing rates of suspended sediment generation were created by changing the amount of sediment generated by streamflow through the parameter α_{QS} and by changing Q_t across all flows for the entire simulation period. Results are shown only for changing α_{QS} because the results for changing Q_t were nearly the same (Fig. 9). At all sites, 2 thresholds in M_t were observed within an average S_t range of 5 to 20 mg/L, centered at ~10 mg/L (Fig. 9). The threshold at ~5 mg/L represents $S_{t,avg}$ where a stable population was no longer resistant to S_t fluctuations, and the threshold at ~20 mg/L represents the $S_{t,avg}$ that each site's population could tolerate before being extirpated. In a comparison of the effect of a more realistic ±10% change at the 3 example sites, only Chippewa (3) is predicted to be responsive to changes in sediment generation rates.

DISCUSSION

The model successfully predicted the spatial variability in M at the watershed scale by accounting for long-term, temporally covarying environmental stressors (i.e., Q, S, C) and their interdependent process interactions despite relatively noisy empirical relationships underlying some functional interactions. Including nonlinear interactions and integrating them over long time periods resulted in much better predictability than either simple

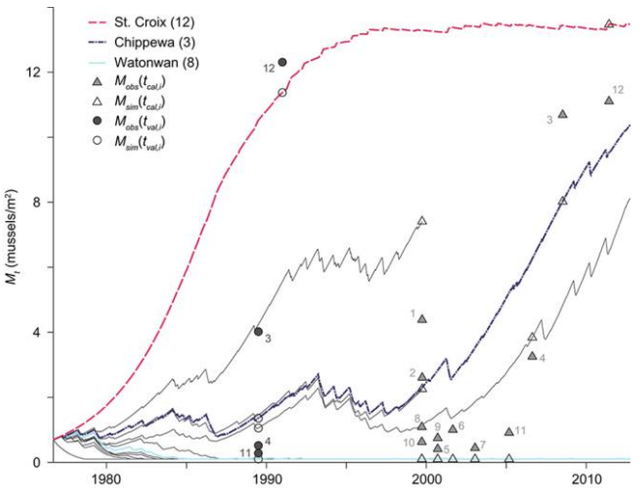

Figure 8. Simulated trajectories of mussel population density (M_t) at all sites over time. Streamflow data for sites 1 and 2 did not extend past year 2000 so these trajectories end accordingly. See Table 2 for site codes.

correlation-type relationships with static variables, or the simplified versions of our model (analysis with static geomorphic and hydraulic variables; Appendix S1). The significant correlation between the streamflow-dependent S_t and the observed M_t supports the hypothesis that S_t and Q_t are 1st-order controls on population density in this system. The additional complexity introduced by considering long-term process dynamics and integrating the effects of all environmental stressors over time through the complete Q–S–C–M model resulted in substantially higher predictive power as seen with both the calibration and validation data sets.

We assumed that long-term temporal dynamics and chronic exposures rather than short-term, catastrophic events, such as scouring or desiccation during drought, control mussel population densities (Strayer et al. 2004, but see Allen et al. 2013, Atkinson et al. 2014). Basins with different land use may exhibit dependencies on variables that are currently not included in the model. However, the model could be extended to include these variables if functional interactions were defined. For instance, fish-host availability and NH_3 concentrations in pore water can be significant stressors in other agricultural systems, and if the dependencies of these stressors on streamflow or other modeled variables were known, then these too could be incorporated (Vaughn and Taylor 2000, Newton et al. 2003, Strayer and Malcom 2012, Cao et al. 2013, Österling and Larsen 2013).

The model also could be used to assess the population density response of a single species to long-term exposure to modeled environmental stressors if sufficient parameterization data were to become available. The generic or site-aggregate mussel concept would still be used to account for the effect of the mussel bed on the stressors through Eq. 8. Responses to modeled stressors, Eqs 13 and 14, would be reparameterized based on the species-specific recruitment response to S_t and, potentially, the specific-species carrying capacity response to food limitation. To our knowledge, this information is currently available for few species. It would be more difficult and perhaps less appropriate to develop the model to be age-specific. Nonphytoplankton food sources, seasonal temperature dependencies, discrete periods of juvenile recruitment, time lags to maturity, and other life-history traits could be included as well, but these variables would increase model complexity and would require additional observations to parameterize the model.

As filter feeders, mussels provide important feedback on the physical and chemical environment by siphoning suspended particulates from the water column, improving water column clarity, and reducing the concentration of suspended solids, which may enhance their own survival (Thorp et al. 1998, Nichols and Garling 2000, Vaughn and Hakenkamp 2001). When the model was run without mussel filtration affecting S_t, population density plummeted to model minima at 10 of 12 sites, a result inconsistent with survey observations. As population density increases, so does the strength of the feedback on the environmental stressor S_t, and the population growth rate required to maintain a stable population is lower. This result suggests

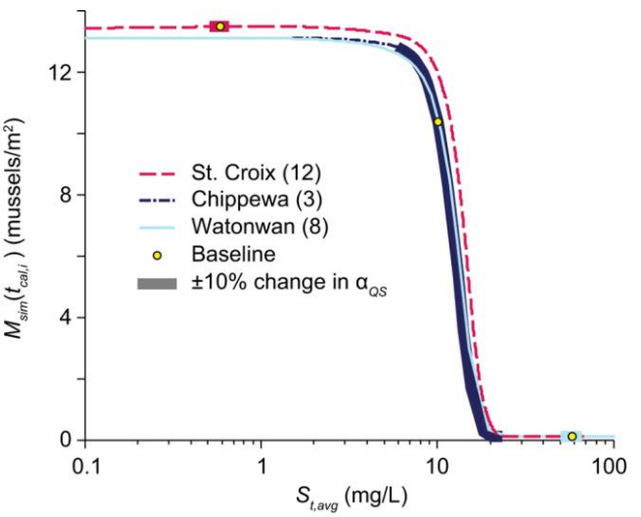

Figure 9. Simulated mussel population density ($M_{sim}[t_{cal,i}]$) response to scenarios of change in suspended sediment generation rate at the 3 example sites (f_1; Eq. 7). Yellow dots show the current daily average sediment concentration, averaged over the model run duration. The thicker line segments correspond to more realistic changes of sediment generation of ±10% α_{QS}.

that at moderate S_t, mussel filtration promotes survival by decreasing environmental stressors and reinforces the concept of mussels as ecosystem engineers (Gutiérrez et al. 2003).

Food limitation effects were predicted by the model at sites with $M_{sim}(t_{cal,i}) > 4$ mussels/m^2 and accounted for as much as a 49% reduction in $M_{sim}(t_{cal,i})$. This result suggests that food limitation occurs at locations with large mussel densities, consistent with previously reported experimental results (Silverman et al. 1997, Kesler et al. 2007, Vaughn et al. 2008). However, in nutrient-rich systems, food resource production may outpace food consumption (Strayer 2013, Hornbach et al. 2014).

Implications for mussel population management

Simulated mussel population densities were in 1 of 3 empirically observed states: extirpation, transitional, or effective (not nominal) carrying capacity (Fig. 6A). For sites with minimal population densities, such as Watonwan (8), even substantial changes in population parameters may not translate into higher densities because of extinction debts or population deficit effects on both recruitment and feed-forward control of suspended sediment (Tilman et al. 1994, Hanski and Ovaskainen 2002, Arvidsson et al. 2012). In contrast, sites with population densities near the effective carrying capacity, such as St Croix (12), may show resilience to increasing streamflow-dependent sediment generation through self-promoting feedback in which mussel filtration decreases S_t. Sites where simulated population densities fall within the transitional region are most responsive to restoration efforts that could enhance juvenile survival and most vulnerable to environmental degradation.

In scenarios of varied suspended sediment generation rates, such as could result from changes in watershed land use, riparian buffer strips or climate change, long-term predicted mussel population densities were in 1 of 3 empirically observed states: extirpation, transitional, or effective carrying capacity (Fig. 9). The population response to $S_{t,avg}$ had 2 thresholds: a threshold where a stable population was no longer resistant to suspended sediment fluctuations (~5 mg/L) and a threshold where populations were extirpated (~20 mg/L). Mussel populations within the transitional region between these 2 thresholds were most sensitive to changing environmental stressors. Small reductions in environmental stressors at these sites are likely to have the largest effect on rehabilitation. For example, among the 3 example sites presented in Fig. 9, Chippewa (3) is predicted to be most responsive to changes in sediment generation rates, and management actions to preserve or restore watershed conditions in this basin are likely to be more effective toward promoting mussel population growth than efforts in St Croix (12) or Watonwan (8) basins. The lower threshold value (~5 mg/L) is lower than the model parameter value governing the initiation of the suspended sediment effect on juvenile recruitment rates (S^*_M = 10 mg/L) and the upper threshold value (~20 mg/L) corresponds to when the effective mussel population growth rate is equal to 0 (S_t = 18.9 mg/L; see Fig. 4C). This threshold response of mussel populations warrants further investigation, including species-specific responses to critical S_t values at these fairly low concentrations. This type of site and population classification can be used to prioritize sites for focused monitoring or management.

Concluding remarks

We have presented a simplified process-interaction model of reach-scale mussel population density that explicitly accounts for the long-term propagation of time-varying environmental stressors (here, suspended sediment and phytoplankton concentration), and we have demonstrated its application in 2 watersheds in the Midwest. The model could be expanded to individual species or other interacting environmental stressors, such as pollutants, substrate instability, and invasive zebra mussels, which could be critical in other systems, provided that sufficient experimental data sets were available to parameterize it. The proposed modeling approach, based on identifying the interdependent functional relationships among dynamic system drivers, provides a means to test whether chronic exposures to environmental stressors may be responsible for ecological decline by integrating mechanistic understanding from the literature to derive process interactions. The high model predictability for both the calibration and validation data sets suggests that the hypothesized primary stressors, i.e., chronic exposure to suspended sediment and food limitation, are indeed 1st-order controls on long-term changes in native mussel population density in this river system. Our model of mussel population density is useful for testing hypotheses of limiting factors, examining the role of feedback loops, identifying priority locations for restoration activities, and evaluating climate- or landuse-change scenarios. Accounting for the effects of long-term, dynamic environmental degradation on freshwater biota, as outlined, can help develop strategies for protection or recovery of at-risk populations struggling against the multifaceted aspects of chronically poor ecological conditions.

ACKNOWLEDGEMENTS

This research was funded by National Science Foundation (NSF) grant EAR-1209402 under the Water Sustainability and Climate Program (WSC): REACH (Resilience under Accelerated Change). The project benefited from collaborations made possible by NSF grant EAR-1242458 under Science Across Virtual Institutes (SAVI): LIFE (Linked Institutions for Future Earth).

We thank Bernard Sietman for the useful discussion and the Minnesota Department of Natural Resources for the mussel data. All programs were coded in Matlab 2012a and are available upon request.

LITERATURE CITED

Alimov, A. F. 1981. Functional ecology of bivalves (Funktzionalnaja Ekologija Presnovodnykh Dvustvorchatykh Molluskov). Nauka Press, Leningrad, Russia.

Allen, D. C., H. S. Galbraith, C. C. Vaughn, and D. E. Spooner. 2013. A tale of two rivers: implications of water management practices for mussel biodiversity outcomes during droughts. Ambio 42:881–891.

Allen, D. C., and C. C. Vaughn. 2010. Complex hydraulic and substrate variables limit freshwater mussel species richness and abundance. Journal of the North American Benthological Society 29:383–394.

Amyot, J. P., and J. Downing. 1997. Seasonal variation in vertical and horizontal movement of the freshwater bivalve *Elliptio complanata* (Mollusca: Unionidae). Freshwater Biology 37: 345–354.

Angel, J., and F. Huff. 1997. Changes in heavy rainfall in Midwestern United States. Journal of Water Resources Planning and Management 123:246–249.

Arbuckle, K. E., and J. A. Downing. 2002. Freshwater mussel abundance and species richness: GIS relationships with watershed land use and geology. Canadian Journal of Fisheries and Aquatic Sciences 59:310–316.

Arvidsson, B. L., J. Karlsson, and M. E. Österling. 2012. Recruitment of the threatened mussel *Margaritifera margaritifera* in relation to mussel population size, mussel density and host density. Aquatic Conservation: Marine and Freshwater Ecosystems 22:526–532.

Atkinson, C. L., A. D. Christian, D. E. Spooner, and C. C. Vaughn. 2014. Long-lived organisms provide an integrative footprint of agricultural land use. Ecological Applications 24:375–384.

Baker, S. M., and D. J. Hornbach. 2001. Seasonal metabolism and biochemical composition of two unionid mussels, *Actinonaias ligamentina* and *Amblema plicata*. Journal of Molluscan Studies 67:407–416.

Berg, D. J., T. D. Levine, J. A. Stoeckel, and B. K. Lang. 2008. A conceptual model linking demography and population genetics of freshwater mussels. Journal of the North American Benthological Society 27:395–408.

Biggs, B. J. F., V. I. Nikora, and T. H. Snelder. 2005. Linking scales of flow variability to lotic ecosystem structure and function. River Research and Applications 21:283–298.

Bright, R., C. Gatenby, R. Heisler, E. Plummer, K. Stramer, and W. Ostlie. 1995. A survey of the mussels of Pomme de Terre and Chippewa Rivers, Minnesota, 1990. Final report for the Minnesota Department of Natural Resources. (Available from: http://www.dnr.state.mn.us/eco/nongame/projects/research_reports)

Bright, R., C. Gatenby, D. Olson, and E. Plummer. 1990. A survey of the mussels of the Minnesota River, 1989. Final report. Minnesota Department of Natural Resources, St Paul, Minnesota. (Available from: http://www.dnr.state.mn.us/eco/nongame/projects/research_reports)

Brim Box, J., and J. Mossa. 1999. Sediment, land use, and freshwater mussels: prospects and problems. Journal of the North American Benthological Society 18:99–117.

Cao, Y., J. Huang, K. S. Cummings, and A. Holtrop. 2013. Modeling changes in freshwater mussel diversity in an agriculturally dominated landscape. Freshwater Science 32:1205–1218.

Carlisle, D. M., D. M. Wolock, and M. R. Meador. 2011. Alteration of streamflow magnitudes and potential ecological consequences: a multiregional assessment. Frontiers in Ecology and the Environment 9:264–270.

Carpenter, S. R., E. H. Stanley, and M. J. Vander Zanden. 2011. State of the world's freshwater ecosystems: physical, chemical, and biological changes. Annual Review of Environment and Resources 36:75–99.

Ceola, S., I. Hödl, M. Adlboller, G. Singer, E. Bertuzzo, L. Mari, G. Botter, J. Waringer, T. J. Battin, and A. Rinaldo. 2013. Hydrologic variability affects invertebrate grazing on phototrophic biofilms in stream microcosms. PloS ONE 8:e60629.

Changnon, B. S. A., and K. E. Kunkel. 1995. Climate-related fluctuations in Midwestern floods during 1921–1985. Journal of Water Resources Planning and Management 121:326–334.

Cuddington, K., M. Fortin, L. Gerber, A. Hastings, A. Liebhold, M. O'Connor, and C. Ray. 2013. Process-based models are required to manage ecological systems in a changing world. Ecosphere 4:1–12.

Culp, J. M., R. B. Brua, G. A. Benoy, and P. A. Chambers. 2013. Development of reference conditions for suspended solids in streams. Canadian Water Resources Journal 38:85–98.

Dadaser-Celik, F., and H. Stefan. 2009. Stream flow response to climate in Minnesota. Report No. 510. St Anthony Falls Laboratory, University of Minnesota, Minneapolis, Minnesota.

Daniel, W. M., and K. M. Brown. 2013. Multifactorial model of habitat, host fish, and landscape effects on Louisiana freshwater mussels. Freshwater Science 32:193–203.

Daraio, J. A., L. J. Weber, T. J. Newton, and J. M. Nestler. 2010. A methodological framework for integrating computational fluid dynamics and ecological models applied to juvenile freshwater mussel dispersal in the Upper Mississippi River. Ecological Modeling 221:201–214.

Donatell, J., C. Klucas, P. Anderson, D. Duffey, B. Monson, G. Flom, J. Chirhart, K. Parson, and D. Christopherson. 2014. Lower St. Croix River watershed monitoring and assessment report. Minnesota Pollution Control Agency document no.: wq-ws3-070300056. Minnesota Pollution Control Agency, Minneapolis, Minnesota. (Available from: Minnesota Pollution Control Agency, 520 Lafayette Road North, St Paul, Minnesota 55155 USA.)

Downing, J. A., P. Van Meter, and D. A. Woolnough. 2010. Suspects and evidence: a review of the causes of extirpation and decline in freshwater mussels. Animal Biodiversity and Conservation 33:151–185.

Engstrom, D. R., J. E. Almendinger, and J. A. Wolin. 2009. Historical changes in sediment and phosphorus loading to the Upper Mississippi River: mass-balance reconstructions from the sediments of Lake Pepin. Journal of Paleolimnology 41:563–588.

Fago, D., and J. Hatch. 1993. Aquatic resources of the St. Croix River basin. Pages 23–56 *in* L. W. Hesse, C. B. Stalnaker, N. G. Benson, and J. R. Zuboy (editors). Proceedings of the Sympo-

sium on Restoration Planning for the Rivers of the Mississippi River Ecosystem. Biological Report 19, October 1993. National Biological Survey, US Department of the Interior, Washington, DC.

French, S. K., and J. D. Ackerman. 2014. Responses of newly settled juvenile mussels to bed shear stress: implications for dispersal. Freshwater Science 33:46–55.

Gangloff, M. M., and J. W. Feminella. 2007. Stream channel geomorphology influences mussel abundance in Southern Appalachian streams, U.S.A. Freshwater Biology 52:64–74.

Gascho Landis, A. M., W. R. Haag, and J. A. Stoeckel. 2013. High suspended solids as a factor in reproductive failure of a freshwater mussel. Freshwater Science 32:70–81.

Geist, J., and K. Auerswald. 2007. Physicochemical stream bed characteristics and recruitment of the freshwater pearl mussel (*Margaritifera margaritifera*). Freshwater Biology 52:2299–2316.

Gutiérrez, J. L., C. G. Jones, D. L. Strayer, and O. O. Iribarne. 2003. Mollusks as ecosystem engineers: the role of shell production in aquatic habitats. Oikos 101:79–90.

Haag, W. R. 2012. North American freshwater mussels: natural history, ecology, and conservation. Cambridge University Press, New York.

Haag, W. R., and J. D. Williams. 2013. Biodiversity on the brink: an assessment of conservation strategies for North American freshwater mussels. Hydrobiologia 735:45–60.

Hanski, I., and O. Ovaskainen. 2002. Extinction debt at extinction threshold. Conservation Biology 16:666–673.

Hornbach, D. J. 1991. Factors influencing the distribution of unionid mussels in the St. Croix River at Franconia, MN. Final report. Minnesota Department of Natural Resources, Minneapolis, Minnesota. (Available from: http://www.dnr.state.mn.us/eco/nongame/projects/research_reports)

Hornbach, D. J. 2001. Macrohabitat factors influencing the distribution and abundance of naiads in the St. Croix River, MN and WI, USA. Pages 213–230 *in* G. Bauer and W. Wachtler (editors). Ecology and evolutionary biology of the freshwater mussels Unionoidea, Ecological Studies Vol. 145. Springer, Berlin, Germany.

Hornbach, D. J., and T. Deneka. 1996. A comparison of a qualitative and a quantitative collection method for examining freshwater mussel assemblages. Journal of the North American Benthological Society 15:587–596.

Hornbach, D. J., M. C. Hove, B. D. Dickinson, K. R. MacGregor, and J. R. Medland. 2010. Estimating population size and habitat associations of two federally endangered mussels in the St. Croix River, Minnesota and Wisconsin, USA. Aquatic Conservation: Marine and Freshwater Ecosystems 20:250–260.

Hornbach, D. J., M. C. Hove, H. T. Liu, F. R. Schenck, D. Rubin, and B. J. Sansom. 2014. The influence of two differently sized dams on mussel assemblages and growth. Hydrobiologia 724:279–291.

Hornbach, D. J., C. M. Way, T. E. Wissingl, and A. J. Burky. 1984. Effects of particle concentration and season on the filtration rates of the freshwater clam, *Sphaerium striatinum* Lamarck (Bivalvia: Pisidiidae). Hydrobiologia 108:83–96.

Howard, J. K., and K. M. Cuffey. 2003. Freshwater mussels in a California North Coast Range river: occurrence, distribution, and controls. Journal of the North American Benthological Society 22:63–77.

Jin, S., L. Yang, P. Danielson, C. Homer, J. Fry, and G. Xian. 2013. A comprehensive change detection method for updating the National Land Cover Database to circa 2011. Remote Sensing of Environment 132:159–175.

Karl, T. R., R. W. Knight, D. R. Easterling, and R. G. Quayle. 1996. Indices of climate change for the United States. Bulletin of the American Meteorological Society 77:279–292.

Kelley, D., and E. Nater. 2000. Source apportionment of lake bed sediments to watersheds in an Upper Mississippi Basin using a chemical mass balance method. Catena 41:277–292.

Kesler, D. H., T. J. Newton, and L. Green. 2007. Long-term monitoring of growth in the Eastern Elliptio, *Elliptio complanata* (Bivalvia: Unionidae), in Rhode Island: a transplant experiment. Journal of the North American Benthological Society 26:123–133.

Kirsch, N., S. Hanson, J. Renard, and P. A. Enblom. 1985. Biological survey of the Minnesota River. Minnesota Department of Natural Resources. Special Publication 139. Minnesota Department of Natural Resources, Minneapolis, Minnesota.

Kryger, J., and H. U. M. Riisgard. 1988. Filtration rate capacities in 6 species of European freshwater bivalves. Oecologia (Berlin) 77:34–38.

Leopold, L. B., M. G. Wolman, and J. P. Miller. 1964. Fluvial processes in geomorphology. W. H. Freeman Publishers, San Francisco, California.

Marañón, E., P. Cermeño, D. C. López-Sandoval, T. Rodríguez-Ramos, C. Sobrino, M. Huete-Ortega, J. M. Blanco, and J. Rodríguez. 2013. Unimodal size scaling of phytoplankton growth and the size dependence of nutrient uptake and use. Ecology Letters 16:371–379.

MPCA (Minnesota Pollution Control Agency). 2013. DNR/MPCA cooperative stream gaging. Minnesota Pollution Control Agency, Minneapolis, Minnesota. (Available from: http://www.dnr.state.mn.us/waters/csg/index.html)

Musser, K., S. Kudelka, and R. Moore. 2009. Minnesota River Basin trends. Water Resources Center, Minnesota State University, Mankato, Minnesota. (Available from: Water Resources Center, Minnesota State University, Mankato, 184 Trafton Science Center South, Mankato, Minnesota 56003 USA.)

Newton, T. J., J. Allran, J. O'Donnell, M. Bartsch, and W. Richardson. 2003. Effects of ammonia on juvenile unionid mussels (*Lampsilis cardium*) in laborabory sediment toxicity tests. Environmental Toxicity and Chemistry 22:2554–2560.

Newton, T. J., S. J. Zigler, J. T. Rogala, B. R. Gray, and M. Davis. 2011. Population assessment and potential functional roles of native mussels in the Upper Mississippi River. Aquatic Conservation: Marine and Freshwater Ecosystems 21:122–131.

Nichols, S. J., and D. Garling. 2000. Food-web dynamics and trophic-level interactions in a multispecies community of freshwater unionids. Canadian Journal of Zoology 78:871–882.

Nielsen, S. L., S. Enríquez, C. M. Duarte, and K. Sand-Jensen. 1996. Scaling maximum growth rates across photosynthetic organisms. Functional Ecology 10:167–175.

Novotny, E. V., and H. G. Stefan. 2007. Stream flow in Minnesota: indicator of climate change. Journal of Hydrology 334:319–333.

Ogilvie, S., and S. Mitchell. 1995. A model of mussel filtration in a shallow New Zealand lake, with reference to eutrophication control. Archiv für Hydrobiologie 133:471–482.

Österling, M. E., B. L. Arvidsson, and L. A. Greenberg. 2010. Habitat degradation and the decline of the threatened mussel *Margaritifera margaritifera*: influence of turbidity and sedimentation on the mussel and its host. Journal of Applied Ecology 47:759–768.

Österling, M. E., and B. M. Larsen. 2013. Impact of origin and condition of host fish (*Salmo trutta*) on parasitic larvae of *Margaritifera margaritifera*. Aquatic Conservation: Marine and Freshwater Ecosystems 23:564–570.

Peterson, J. T., J. M. Wisniewski, C. P. Shea, and C. R. Jackson. 2011. Estimation of mussel population response to hydrologic alteration in a southeastern U.S. stream. Environmental Management 48:109–122.

Poff, N. L., and J. K. H. Zimmerman. 2010. Ecological responses to altered flow regimes: a literature review to inform the science and management of environmental flows. Freshwater Biology 55:194–205.

Poole, K. E., and J. A. Downing. 2004. Relationship of declining mussel biodiversity to stream-reach and watershed characteristics in an agricultural landscape. Journal of the North American Benthological Society 23:114–125.

Power, M. E., A. Sun, G. Parker, W. E. Dietrich, and J. T. Wootton. 1995. Hydraulic food-chain models. BioScience 45:159–167.

Pusch, M., J. Siefert, and N. Walz. 2001. Filtration and respiration rates of two unionid species and their impact on the water quality of a lowland river. Pages 317–326 *in* G. Bauer and K. Wachtler (editors). Evolution of the freshwater mussels Unionoida. Springer–Verlag Berlin, Heidelberg, Germany.

Ricciardi, A., and J. B. Rasmussen. 1999. Extinction rates of North American freshwater fauna. Conservation Biology 13:1220–1222.

Sarnelle, O. 1992. Nutrient enrichment and grazer effects on phytoplankton in lakes. Ecology 73:551–560.

Schallenberg, M., and C. W. Burns. 2004. Effects of sediment resuspension on phytoplankton production: teasing apart the influences of light, nutrients and algal entrainment. Freshwater Biology 49:143–159.

Schottler, S. P., J. Ulrich, P. Belmont, R. Moore, J. W. Lauer, D. R. Engstrom, and J. E. Almendinger. 2014. Twentieth century agricultural drainage creates more erosive rivers. Hydrological Processes 28:1951–1961.

Silverman, H., S. J. Nichols, J. S. Cherry, E. Achberger, J. W. Lynn, and T. H. Dietz. 1997. Clearance of laboratory-cultured bacteria by freshwater bivalves: differences between lentic and lotic unionids. Canadian Journal of Zoology 75:1857–1866.

Smith, D. R. 2006. Survey design for detecting rare freshwater mussels. Journal of the North American Benthological Society 25:701–711.

Stefan, H. G., J. J. Cardoni, F. R. Schiebe, and C. M. Cooper. 1983. Model of light penetration in a turbid lake. Water Resources Research 19:109–120.

Stein, B., L. Kutner, and J. Adams (editors). 2000. Precious heritage: the status of biodiversity in the United States. Oxford University Press, New York.

Steuer, J. J., T. J. Newton, and S. J. Zigler. 2008. Use of complex hydraulic variables to predict the distribution and density of unionids in a side channel of the Upper Mississippi River. Hydrobiologia 610:67–82.

Strayer, D. L. 2008. Freshwater mussel ecology: a multifactor approach to distribution and abundance. University of California Press, Berkeley, California.

Strayer, D. L. 2013. Understanding how nutrient cycles and freshwater mussels (Unionoida) affect one another. Hydrobiologia 735:277–292.

Strayer, D. L., J. A. Downing, W. R. Haag, T. L. King, J. B. Layzer, T. J. Newton, and S. J. Nichols. 2004. Changing perspectives on pearly mussels, North America's most imperiled animals. BioScience 54:429–439.

Strayer, D. L., and H. M. Malcom. 2012. Causes of recruitment failure in freshwater mussel populations in southeastern New York. Ecological Applications 22:1780–1790.

Thorp, J. H., D. Delong, and K. S. Greenwood. 1998. Isotopic analysis of three food web theories in constricted and floodplain regions of a large river. Oecologia (Berlin) 117:551–563.

Tilman, D. G., R. M. May, C. L. Lehman, and M. A. Nowak. 1994. Habitat destruction and the extinction debt. Nature 371:65–66.

USGS (US Geological Survey). 2014. USGS water data for Minnesota. US Geological Survey, Reston, Virginia. (Available from: http://waterdata.usgs.gov/mn/nwis)

Vaughn, C., and C. Hakenkamp. 2001. The functional role of burrowing bivalves in freshwater ecosystems. Freshwater Biology 46:1431–1446.

Vaughn, C. C., S. J. Nichols, and D. E. Spooner. 2008. Community and foodweb ecology of freshwater mussels. Journal of the North American Benthological Society 27:409–423.

Vaughn, C. C., and C. M. Taylor. 2000. Macroecology of a host-parasite relationship. Ecography 23:11–20.

Watters, G. T., S. H. O'Dee, and S. Chordas. 2001. Patterns of vertical migration in freshwater mussels (Bivalvia: Unionoida). Journal of Freshwater Ecology 16:541–549.

Zigler, S. J., T. J. Newton, J. J. Steuer, M. R. Bartsch, and J. S. Sauer. 2007. Importance of physical and hydraulic characteristics to unionid mussels: a retrospective analysis in a reach of large river. Hydrobiologia 598:343–360.